MATERIALE PLASTICE
https://revmaterialeplastice.ro
https://doi.org/10.37358/Mat.Plast.1964

Experimental Investigation for the Prediction of Surface Roughness Height Parameters in Abrasive Water Jet Cutting of Kevlar/epoxy Composites

DINU-VALENTIN GUBENCU*
Politehnica University of Timisoara, Mechanical Engineering Faculty, Mechanical Machines, Equipment and Transportation Department, 1 Mihai Viteazul Str., 300222, Timisoara, Romania

Abstract: *The main objective of the research was to study the influence of the abrasive water jet cutting (AWJC) parameters on the surface roughness parameters Rz1max and Rt, obtained when processing Kevlar fiber-reinforced polymers (KFRP). For this purpose, a full factorial experimental program was designed and roughness evaluations were carried out in two different zones of the cut slot. In this way, it was possible to test the statistical significance of the input parameters effects and characterize both these regions, by means of prediction models proposed for each roughness parameter. Finally, response surfaces and level curves were represented to facilitate the selection of proper factors combination to achieve surface finish requirements.*

Keywords*: Kevlar/epoxy composite material, abrasive water jet cutting, total height of the roughness profile, maximum roughness depth, full factorial experiment*

1. Introduction

Kevlar® refers to para-aramid synthetic fibers developed by Dupont™, which features as reinforcement of composite materials an exceptional combination of properties, such as high strength-to-weight ratio, high resistance to impact, cracking and abrasion, low thermal expansion, toughness and moderate stiffness, higher than glass fiber-reinforced composites (GFRP) and much lower than carbon fiber-reinforced composites (CFRP) [1, 2].

Being five times stronger than steel on an equal weight basis, Kevlar® is currently used in a broad range of high-technology applications, in the fields of transport, military or consumer goods. Thanks to the previously mentioned properties, due both to its internal rod-like molecular structure and tight knitting of fibers [1, 2], typical end uses of Kevlar® as structural composite material or dry fabric are for manufacture of automotive components - brake pads, clutches, gaskets, hoses and belts reinforcements, battery separators, race car bodies and air dams - , aircraft components - engine nacelles, cabin flooring and interiors -, shipping components - hulls, kayaks, canoes, surfboards, sail cloth - , military components - bulletproof vests, tank armor, helmets, aircraft radomes - , vehicles tires, protective clothing, ropes, optical cables (Figure 1) [2-6].

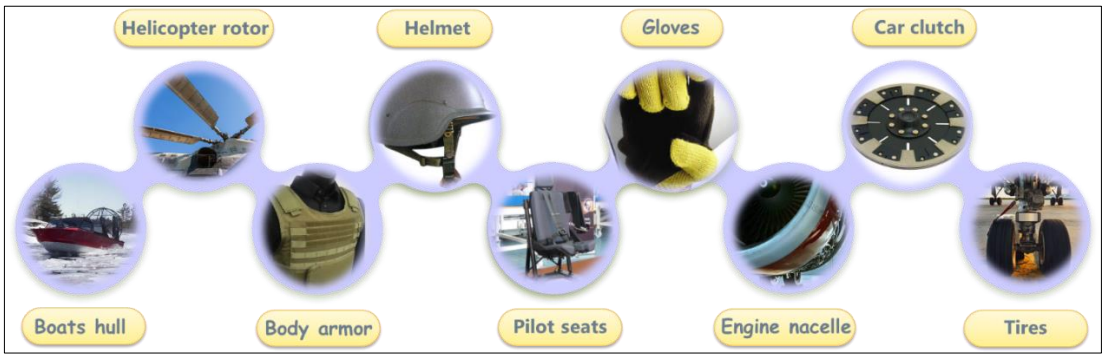

Figure 1. Kevlar® fibers applications [2–6]

email: email: dinu.gubencu@upt.ro

The widespread use of KFRP in the formerly mentioned high performance applications led to the necessity to identify more efficient and effective processing methods, since this material is difficult-to-machine by means of classical processes. Thus, nonconventional technologies, like AWJC, have become a natural option. Within AWJC process, the erosive effect is ensured by the abrasive material, which acts on the workpiece as an abrasive and water mixture, forming a coherent jet. The water jet roles in the process are to accelerate the abrasive particles and to evacuate both eroded and wear products [7]. The most important advantages of the AWJC are high flexibility and efficiency, high precision and accuracy of processed parts, absence of thermal distortion.

To analyze the possibilities of prediction or optimization of the AWJC process, it is useful to carry out a systemic study, as was seen in case of other technological processes too [8-10]. The specific technological transformations that occur during AWJC involve the directed or controlled unfolding of complex and diffuse phenomenological processes. Considering AWJC process as a cybernetic system (Figure 2), three structural sets of associated variables can be defined:

- input variables, representing the factors that initiate technological transformations;
- process variables, which assure the progress of technological makeovers;
- output variables, known also as objective functions, which characterize the performance of AWJC process.

Within the category of input variables (Figure 2), which act to determine the achievement of required transformations, two subsets can be identified:

- structural variables, including quantitative as well as qualitative factors, determined by the constructive particularities of the AWJC equipment subsystems and the requirements related to the workpieces material, geometry and precision;

- operating variables, exclusively quantitative factors selected in accordance with the preceding variables, which can be easily adjusted to meet product specifications.

The effective technological transformations are assessed by means of some technological performance indicators, which refer to the processed part:

- dimensional and geometrical accuracy and precision, quantified by deviations, ε_d, ε_g, among which the most frequently used is kerf taper angle k_θ;

- surface finish, quantitatively evaluated by different roughness parameters, *Ra*, *Rz*, *Rt*, *Rz1max*.

Since a certain transformation can be produced with different speeds and energy consumption, therefore implicitly with different costs depending on the conditions of implementation, process technological and technical-economic indicators are also considered, being important only as decision criteria. Thus, process productivity, respectively production costs, are measured by the objective functions presented in Figure 2. Moreover, some unwanted transformations may occur, like delamination of the part, or caused by different wear processes, which may require a quantitative assessment.

It is well known that material removal rate is the main goal, especially in roughing operations, meanwhile dimensional and geometrical accuracy or precision, surface finish are usually of secondary importance. On the other hand, when performing finishing operations, the priorities are quite opposite. Thus, in many cases defining and analyzing global performance indicators for assessing both efficiency and effectiveness of AWJC process may be very useful. These global indicators are expressed by ratios, individual parameters being considered at numerator or denominator, according to their target of improvement. Hence, one of the following indicators can be chosen:

$$PI_1 = \frac{Q_c}{Rt} \tag{1}$$

$$PI_2 = \frac{Q_c}{Rt \cdot k_a} \tag{2}$$

$$PI_3 = \frac{Q_c}{Rt \cdot k_a \cdot p_w} \tag{3}$$

$$PI_4 = \frac{Q_c}{Rt \cdot k_a \cdot p_w \cdot q_a} \tag{4}$$

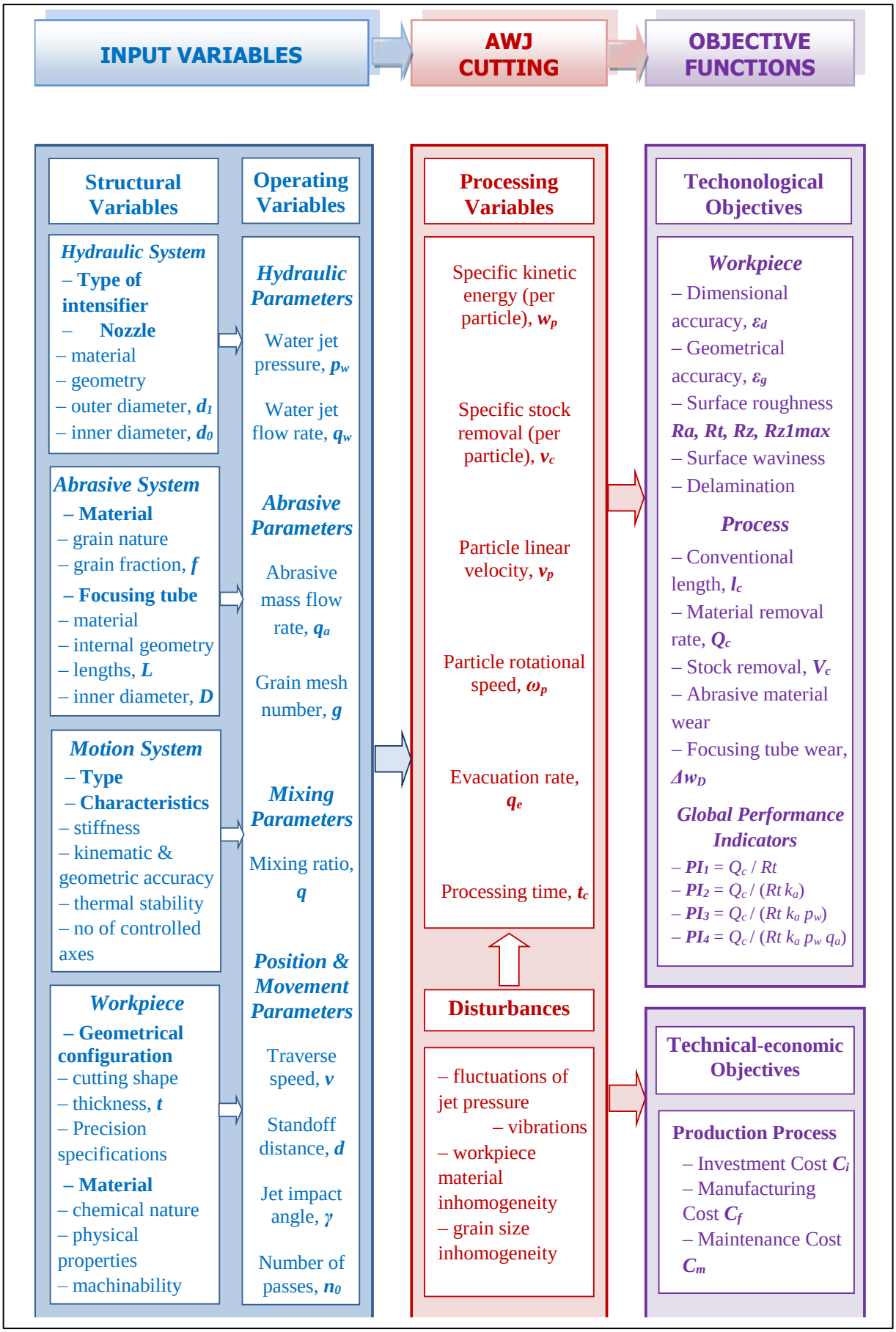

Figure 2. Cybernetic model of AWJC process

As can be seen, all these complex objective functions include material removal rate, Q_c, and a proper roughness parameter, for example in equations (1…4), total height roughness, *Rt*. Also, kerf taper angle, k_a, for a more complete evaluation of process accuracy, water pressure, p_w, as a measure of energy consumption, and abrasive mass flow rate, q_a, as a measure of abrasive consumption, may be introduced in relations too.

Process performance, described by the objective functions, depend on the input variables directly, and in some cases, also on the processing variables. Therefore, the problem arises of establishing the suitable values of the input parameters that ensure the achievement of the imposed technological or technical-economic objectives. Due to the fact that technological systems depend on various factors having a partially stochastic behavior, these dependencies are difficult to establish by analytical identification, based on knowledge of physical phenomena. Thus, many researches aim to find empirical mathematical models that indicate the relationship between an objective function and the input variables, especially the operating variables.

In case of AWJC of polymer matrix composites with various reinforcements, most studies focused on experimental investigation of surface roughness parameter *Ra* [11–17], kerf taper angle or kerf width [13–17] and material removal rate [18, 19]. Regarding surface finish, almost all researches concluded that it can be improved with increase of water jet pressure, p_w, and drop of the traverse speed, *v*. Other tested input parameters, like abrasive mass flow rate, q_a, or standoff distance, *d*, had a minor or contradictory influence on *Ra* parameter.

All drawn conclusion have a limited validity, depending on material type and thickness, experimental ranges or fixed values of input parameters. Thus, the main objective of the present study was to model the action of selected influence factors on kerf surface finish, obtained after AWJC of KFRP.

2. Materials and methods

2.1. Specimen preparation and measurement

The material under experimental investigation was a Kevlar/epoxy composite laminate, formed using plain weave prepregs by Duqueine Composites, for the ballistic protection of pilot seats (Figure 1). The steps performed for specimen preparation and cut surface inspection are shown in Figure 3. The key characteristics regarding the material are summarized in Table 1.

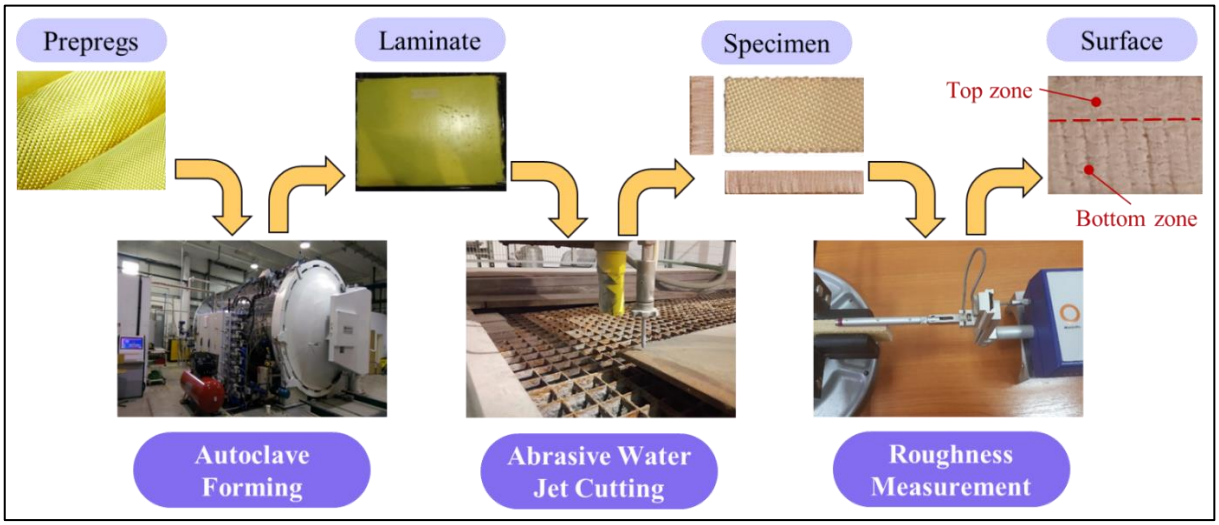

Figure 3. Steps of specimen preparation and investigation

Rectangular shape samples (60 mm x 30 mm) were cut in a single pass with a CNC controlled JEDO AWJC equipment, having the main subassemblies shown in Figure 4. The processing was carried out with different combinations of input parameters, chosen according to the experimentation strategy. At the same time, some of the input variables were kept fixed during AWJC (Table 2).

Table 1. Material features

Fabric		Autoclave Forming		Laminate	
Characteristic	Specification	Characteristic	Specification	Characteristic	Specification
Composition	100% Kevlar 29	Temperature	150°C	No of layers	18
Warp / Weft	3300 / 3300 dtex	Time	240 min.	Resin content	40 %
Density	440 ± 10 g/m^2	Pressure	2±0.5 bar	Thickness	9.5 ± 0.1 mm

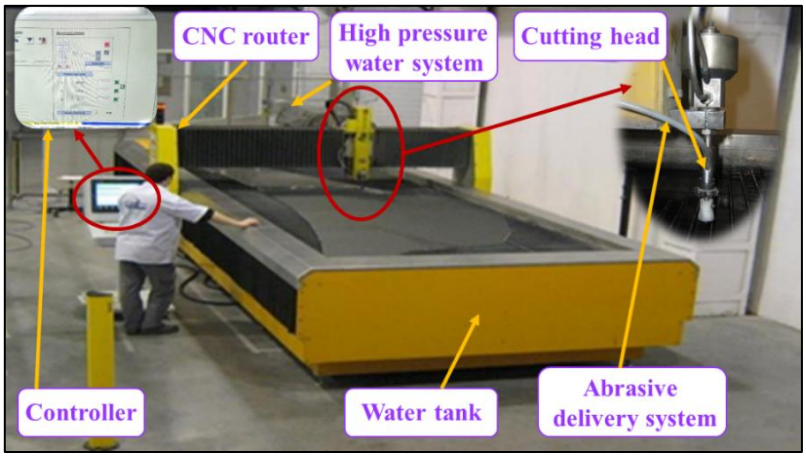

Figure 4. JEDO AWJC equipment

Table 2. Fixed input parameters values

Input Parameter	Specification
Water pressure, p_w [MPa]	300
Water nozzle diameter, d_0 [mm]	0.33
Standoff distance, d [mm]	3
Jet angle of attack, γ [deg.]	90
Abrasive material	garnet

Surface roughness measurement were accomplished with a Taylor-Hobson Surtronic 25 stylus tester (Figure 5). Measurements took place for both characteristic areas of the kerf, namely top zone and bottom zone (Figure 3), keeping for the further data processing only the maximum measured value obtained under the same cutting conditions, chosen from two measurements performed on each surface of samples.

Figure 5. Surface roughness measurement procedure

2.2. Experimental methodology

The most commonly used parameter for specification and evaluating surface finish is the arithmetical mean roughness value, *Ra*, which offers the advantages of easy and repeatable measurements. On the

other hand, *Ra* is almost not influenced by the individual profile features – peaks or valleys – and, as a result, for assessing more completely the functionality of the surfaces, more sensitive parameters to these extreme variations, must be taken into account.

Thus, as objective functions for the present research, the surface roughness parameters significantly influenced by individual deviations were considered [20]:

a. Maximum roughness depth, *Rz1max*, define as the largest of the Rz_i values, corresponding to each of the five sampling lengths lr_i within the evaluation length *ln* (*Rz1max* ≡ Rz_3 in Figure 6);

b. Total height of the roughness profile, *Rt*, calculated as the difference between the highest peak and the deepest valley within the evaluation length *ln* (Figure 6).

It can be accepted, considering the significance of these parameters, that both are designated as roughness height parameters. Also, according to the previous definitions, the maximum value of *Rz1max* may equal the *Rt* value.

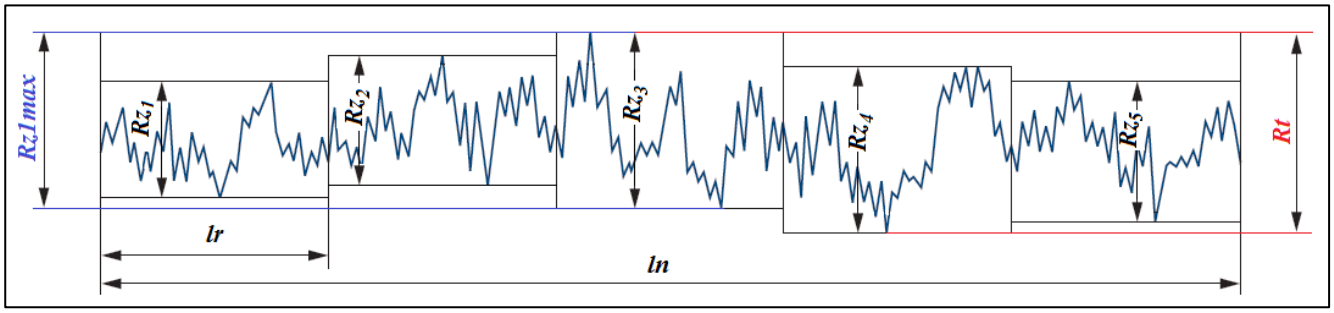

Figure 6. Definition of surface roughness parameters *Rz1max* and *Rt*

These selected parameters offer the possibility to detect some anomalies like burrs and scratches, which cannot be highlighted by measuring only *Ra* [21]. Moreover, although there are several conversion tables or charts between different roughness parameters, the resulting values might vary by up to 25%, according to the considered source. This proves once more the correctness of the decision to model the action of AWJC input factors on these roughness height parameters.

In order to achieve this established objective, a full factorial experiment was designed and performed, involving four input variables: traverse speed, *v*, focusing tube diameter, *D*, abrasive mass flow rate, q_a, and abrasive grain size, *g*.

In addition, a virtual factor was considered, namely the kerf zone, *Z*, targeting to obtain a unified model for both smooth and rough regions, located at the top and bottom of the cut, respectively. So, finally a five-factor full factorial experiment was carried out.

The factors experimental ranges (Table 3) were selected taking into account both the efficiency requirements of the KFRP laminate industrial AWJC and some limitations related to abrasive consumption or available focusing tube diameters of the equipment. Also, a secondary goal was to investigate the influence of using fine (100 mesh #) and ultra-fine (200 mesh #) abrasive grain size, *g*, on surface roughness height parameters.

Table 3. Multifactorial experimental range

Factors	**Coded Values**	**Natural Values**				
		A: *v* [mm/min]	**B: *D*** [mm]	**C: q_a** [g/min]	**D: *g*** [mesh #]	**E: *Z*** [-]
Central Point	0	300	–	180	150	–
Range of variation	Δ_j	200	0.12	20	50	–
Lower Level	–1	100	0.76	160	100	top
Higher Level	+1	500	1.00	200	200	bottom

Factorial experiments are more efficient than one-at-a-time experiments, because the influence of each factor on the objective function is assessed using all experimental runs. Moreover, another

comparative advantage of the factorial treatment structure is the possibility to estimate not only main effects, but interactions too [22].

3. Results and discussions

3.1. Experimental design and results

Measured values and computed average at each run for both roughness parameters investigated are shown in Table 4.

Table 4. Experimental matrix and measured values of roughness parameters *Rz1max* and *Rt*

Run No *i*	A: *v*		B: *D*		C: q_a		D: *g*		E: *Z*		*Rz1max* [µm]			*Rt* [µm]		
	coded	[mm/ min]	coded	[mm]	coded	[g/min]	coded	[mesh #]	coded	[–]	$Rz1max_1$	$Rz1max_2$	$\overline{Rz1max}$	Rt_1	Rt_2	$\overline{Rt}$
1	–1	100	–1	0.76	–1	160	–1	100	–1	top	47	51	49	47	54	50.5
2	+1	500	–1	0.76	–1	160	–1	100	–1	top	77	73	75	81	76	78.5
3	–1	100	+1	1.00	–1	160	–1	100	–1	top	71	66	68.5	73	74	73.5
4	+1	500	+1	1.00	–1	160	–1	100	–1	top	90	103	96.5	92	106	99
5	–1	100	–1	0.76	+1	200	–1	100	–1	top	46	50	48	49	50	49.5
6	+1	500	–1	0.76	+1	200	–1	100	–1	top	81	71	76	81	73	77
7	–1	100	+1	1.00	+1	200	–1	100	–1	top	66	71	68.5	74	71	72.5
8	+1	500	+1	1.00	+1	200	–1	100	–1	top	98	92	95	98	94	96
9	–1	100	–1	0.76	–1	160	+1	200	–1	top	46	46	46	50	48	49
10	+1	500	–1	0.76	–1	160	+1	200	–1	top	73	78	75.5	73	82	77.5
11	–1	100	+1	1.00	–1	160	+1	200	–1	top	52	58	55	60	62	61
12	+1	500	+1	1.00	–1	160	+1	200	–1	top	89	88	88.5	91	88	89.5
13	–1	100	–1	0.76	+1	200	+1	200	–1	top	46	44	45	48	45	46.5
14	+1	500	–1	0.76	+1	200	+1	200	–1	top	70	73	71.5	70	79	74.5
15	–1	100	+1	1.00	+1	200	+1	200	–1	top	58	71	64.5	58	71	64.5
16	+1	500	+1	1.00	+1	200	+1	200	–1	top	104	92	98	106	94	100
17	–1	100	–1	0.76	–1	160	–1	100	+1	bottom	90	92	91	94	97	95.5
18	+1	500	–1	0.76	–1	160	–1	100	+1	bottom	98	124	111	104	124	114
19	–1	100	+1	1.00	–1	160	–1	100	+1	bottom	113	107	110	115	110	112.5
20	+1	500	+1	1.00	–1	160	–1	100	+1	bottom	127	139	133	141	139	140
21	–1	100	–1	0.76	+1	200	–1	100	+1	bottom	88	90	89	88	92	90
22	+1	500	–1	0.76	+1	200	–1	100	+1	bottom	94	91	92.5	94	96	95
23	–1	100	+1	1.00	+1	200	–1	100	+1	bottom	105	113	109	111	113	112
24	+1	500	+1	1.00	+1	200	–1	100	+1	bottom	154	168	161	168	168	168
25	–1	100	–1	0.76	–1	160	+1	200	+1	bottom	95	98	96.5	120	102	111
26	+1	500	–1	0.76	–1	160	+1	200	+1	bottom	101	113	107	110	131	120.5
27	–1	100	+1	1.00	–1	160	+1	200	+1	bottom	82	100	91	84	100	92
28	+1	500	+1	1.00	–1	160	+1	200	+1	bottom	110	124	117	116	138	127
29	–1	100	–1	0.76	+1	200	+1	200	+1	bottom	96	97	96.5	99	97	98
30	+1	500	–1	0.76	+1	200	+1	200	+1	bottom	98	98	98	100	102	101
31	–1	100	+1	1.00	+1	200	+1	200	+1	bottom	107	99	103	110	100	105
32	+1	500	+1	1.00	+1	200	+1	200	+1	bottom	136	109	122.5	136	114	125

The experiment was designed and analyzed using the statistical software Statgraphics Centurion XVI. For a full factorial experiment 2^5, the matrix designed has 32 runs, obtained with all possible combinations of factors levels. Practically, in the matrix columns, the 2 levels of factor *p* were alternated after a number of trials equal to 2^{p-1}. The experimental error estimation, implied the replication of the whole experiment.

In fact, the aim of the conducted experiment was to find, based on measured data, the regression coefficients, b_0, b_j, b_{jk}, of the polynomial, for both investigated roughness parameters [22]:

$$y = b_0 + \sum_{j=1}^{p} b_j x_j + \sum_{j,k=1,\ j\neq k}^{p} b_{jk} x_j x_k, \qquad p = 5, \tag{5}$$

where x_j, x_k – input variables.

3.2. Estimation of regression coefficients and model analysis

The estimated effects on roughness parameters of selected factors and interactions, in decreasing order of importance, are presented in Pareto charts (Figure 7).

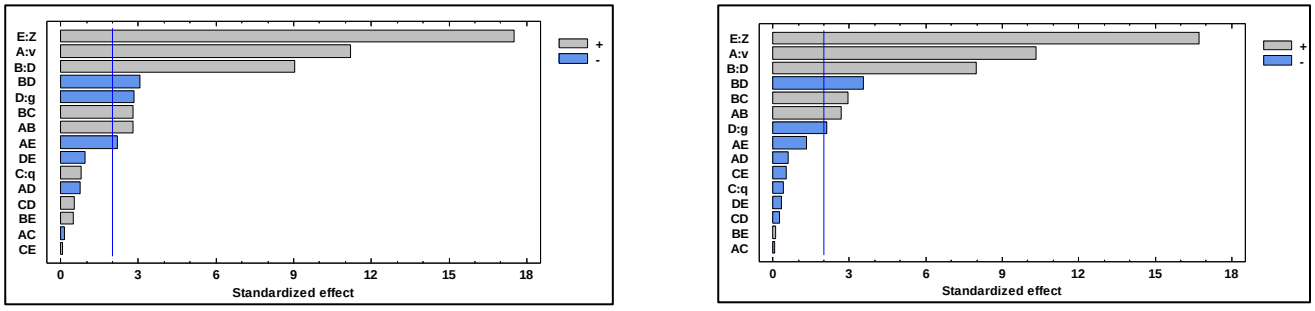

Figure 7. Standardized Pareto chart for roughness parameters (**a.** *Rz1max*, **b.** *Rt*)

The experimental results confirm the existence of the two kerf zones, having different roughness height parameters, identified in previous researches carried out on different types of materials [11, 17]. The ranking of the effects (Figure 7) indicates kerf zone, *Z*, as the factor that exerted the greatest influence on both investigated roughness parameters.

Among the operating variables, the greatest influence, also on both roughness parameters, is exerted by the traverse speed, *v*, followed by the focusing tube diameter, *D*, the decrease of both factors determining a positive effect, of improving surface finish. These effects can be explained, on one hand, by the increase of the impact energy flow in the working space with traverse speed decreasing, and, on the other hand, by the increase of the specific energy, per unit area, for low values of focusing tube diameter.

The use of ultrafine garnet, having a high mesh #, *g*, revealed a positive effect on both roughness height parameters, especially on *Rz1max*, but with a lower magnitude, comparing with previous mentioned factors. Smoother cut surfaces are obtained due to the increased number of particles striking the target area of the workpiece, generating closer erosion trajectories.

Basically, when integrated in factorial experiment, Analysis of Variance (ANOVA) is an algorithm for partitioning variability of measured data, depending on the source causing the variation. In fact, ANOVA tests, using Fisher ratio, the statistical significance of each effect by comparing the mean square against an estimate of the experimental error [22].

ANOVA (Table 5) proves that 4 factors effects and 4 interactions, having *P*-values less than 0.05, exerted a significantly statistical influence on *Rz1max* roughness parameter, at the 95.0% confidence level. Also, in the case of *Rt* roughness parameter, 4 factors effects and 3 interactions have *P*-values less than 0.05, indicating that they are significantly different from zero, at the 95.0% confidence level.

ANOVA proved that abrasive flow rate, q_a, had a statistically insignificant effect on both roughness parameters, at the 95.0% confidence level, for the chosen experimental range. On the other hand, the interaction of this factor with focusing tube diameter turned out to be statistically significant, at 95.0% confidence level. This means that an increased abrasive flow rate, q_a, emphasis negative influence of a higher focusing tube diameter, *D*.

Excluding from the models the interactions that had insignificant effects on roughness parameters, the regression equations fitted to the experimental data, for coded values of input variables, are:

$$Rz1max\ (\mu m) = 89.015 + 12.109\ v + 9.796\ D + 0.859\ q_a - 3.046\ g + 18.984\ Z + 3.015\ v\ D - 2.359\ v\ Z + 3.015\ D\ q_a - 3.328\ D\ g \quad (6)$$

$$Rt\ (\mu m) = 92.671 + 12.484\ v + 9.671\ D - 0.515\ q_a - 2.546\ g + 20.234\ Z + 3.234\ v\ D + 3.546\ D\ q_a - -4.296\ D\ g \quad (7)$$

Table 5. Analysis of variance

ANOVA for *Rz1max*						ANOVA for *Rt*					
Source	**Sum of Squares**	**Df**	**Mean Square**	**F-Ratio**	**P-value**	**Source**	**Sum of Squares**	**Df**	**Mean Square**	**F-Ratio**	**P-value**
A:*v*	9384.77	1	9384.77	124.95	0.0000	A:*v*	9975.02	1	9975.02	106.30	0.0000
B:*D*	6142.64	1	6142.64	81.78	0.0000	B:*D*	5986.89	1	5986.89	63.80	0.0000
C:q_a	47.2656	1	47.2656	0.63	0.4316	C:q_a	17.0156	1	17.0156	0.18	0.6722
D:*g*	594.141	1	594.141	7.91	0.0072	D:*g*	415.141	1	415.141	4.42	0.0408
E:Z	23066.0	1	23066.0	307.10	0.0000	E:Z	26203.5	1	26203.5	279.24	0.0000
AB	582.016	1	582.016	7.75	0.0077	AB	669.516	1	669.516	7.13	0.0104
AC	1.89063	1	1.89063	0.03	0.8746	AC	0.39062	1	0.39062	0.00	0.9488
AD	43.8906	1	43.8906	0.58	0.4484	AD	34.5156	1	34.5156	0.37	0.5471
AE	356.266	1	356.266	4.74	0.0345	AE	159.391	1	159.391	1.70	0.1988
BC	582.016	1	582.016	7.75	0.0077	BC	805.141	1	805.141	8.58	0.0052
BD	708.891	1	708.891	9.44	0.0035	BD	1181.64	1	1181.64	12.59	0.0009
BE	17.0156	1	17.0156	0.23	0.6363	BE	0.76562	1	0.76562	0.01	0.9284
CD	19.1406	1	19.1406	0.25	0.6160	CD	5.64063	1	5.64063	0.06	0.8074
CE	0.390625	1	0.390625	0.01	0.9428	CE	26.2656	1	26.2656	0.28	0.5993
DE	66.0156	1	66.0156	0.88	0.3533	DE	11.3906	1	11.3906	0.12	0.7291
blocks	102.516	1	102.516	1.36	0.2486	blocks	37.5156	1	37.5156	0.40	0.5303
Total error	3530.11	47	75.1087			Total error	4410.36	47	93.8374		
Total (corr.)	45245.0	63				Total (corr.)	49940.1	63			

The *R*-Squared statistic, computed through ANOVA, indicates that the model (6) as fitted explains 92.19 % of the variability in *Rz1max*, and the equation (7) describes 91.16 % of the variability in *Rt*, respectively. Also, Figure 8 shows a good consensus between model predictions and experimental values, proving that each model is an adequate approximation to the true mean structure of the data.

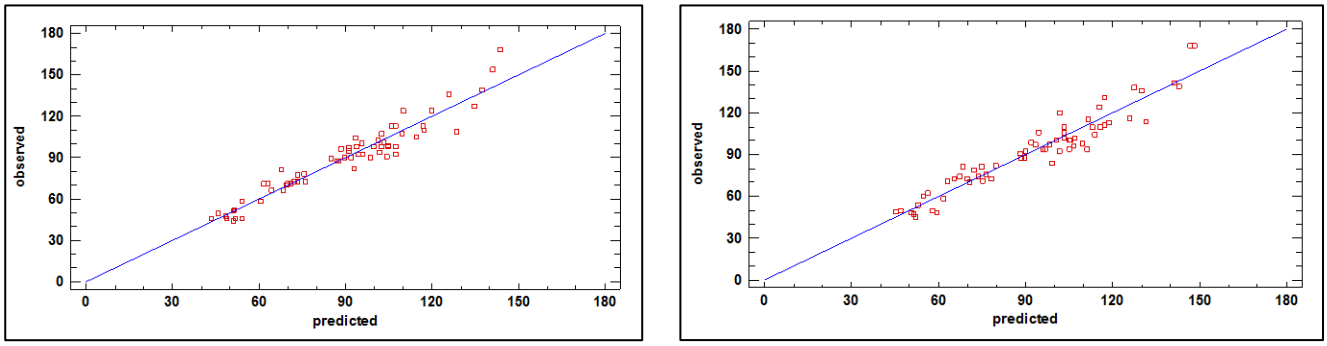

A b

Figure 8. Plot of observed vs predicted values (**a.** *Rz1max*, **b.** *Rt*)

3.3. Response surfaces and level curves

Applying a response surface design methodology, surface plots and level curves for both roughness height parameters were represented. First, regression coefficients of the two models were estimated for natural values of the predictor variables, unlike the previous models, determined for coded values of these variables.

Surface plots can be represented choosing two influence factors each, and setting constant values of interest for the other factors. Such examples are given in Figure 9, for maximum roughness depth, *Rz1max*, and Figure 10, for total height of the roughness profile, *Rt*, for both characteristic regions of the kerf.

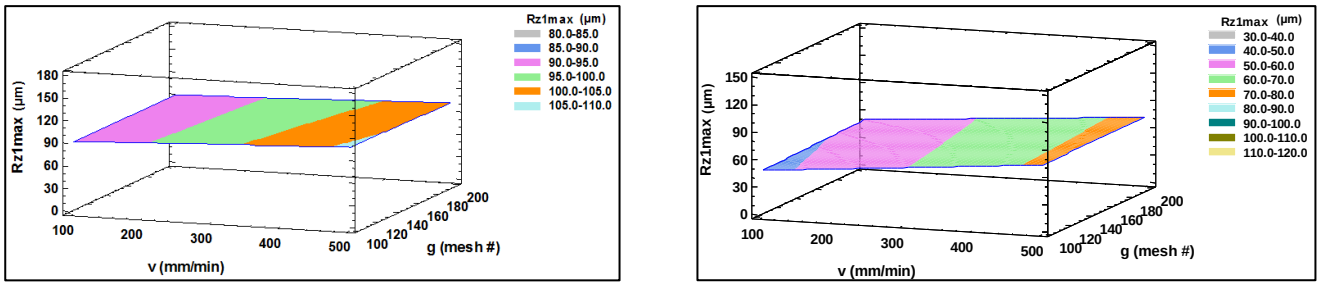

a b

Figure 9. Estimated response function *Rz1max* versus *v* and *g* at *D* = 0.76 mm and q_a = 180 g/min (**a.** bottom zone, **b.** top zone)

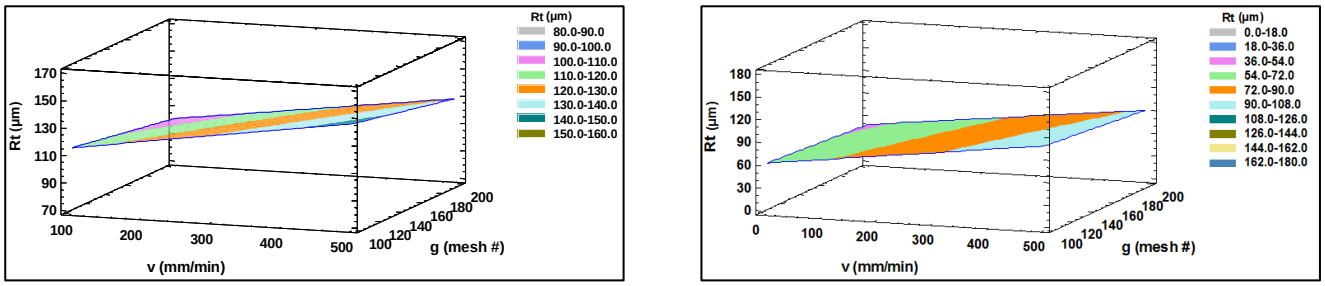

a b

Figure 10. Estimated response function *Rt* versus *v* and *g* at *D* = 1.00 mm and q_a = 180 g/min (**a.** bottom zone, **b.** top zone)

Level curves represent sets of input variables that determine the same expected response [22]. These plots facilitate an easy selection of appropriate combinations of the process parameters, in order to accomplish the specifications of the roughness height parameters.

Examples of level curves for maximum roughness depth, *Rz1max*, are shown in Figure 11, and for total height of the roughness profile, *Rt*, in Figure 12, for both top zone and bottom zone of the cut.

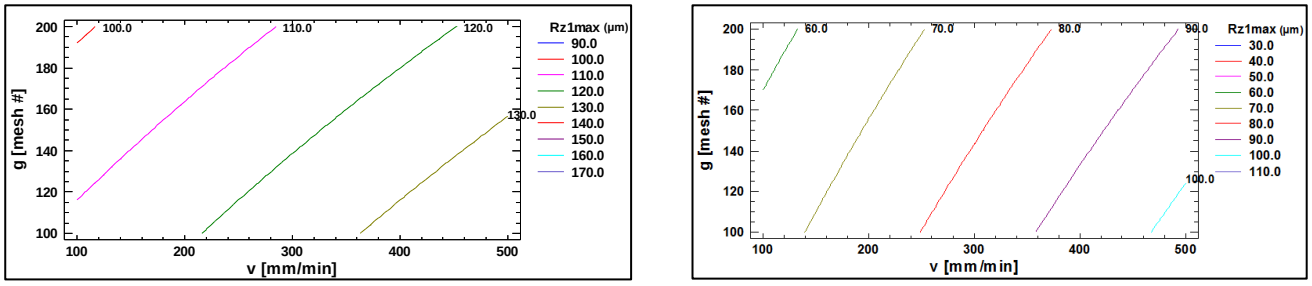

a b

Figure 11. Constant level curves *Rz1max* versus *v* and *g* at *D* = 1.00 mm and q_a = 180 g/min (**a.** bottom zone, **b.** top zone)

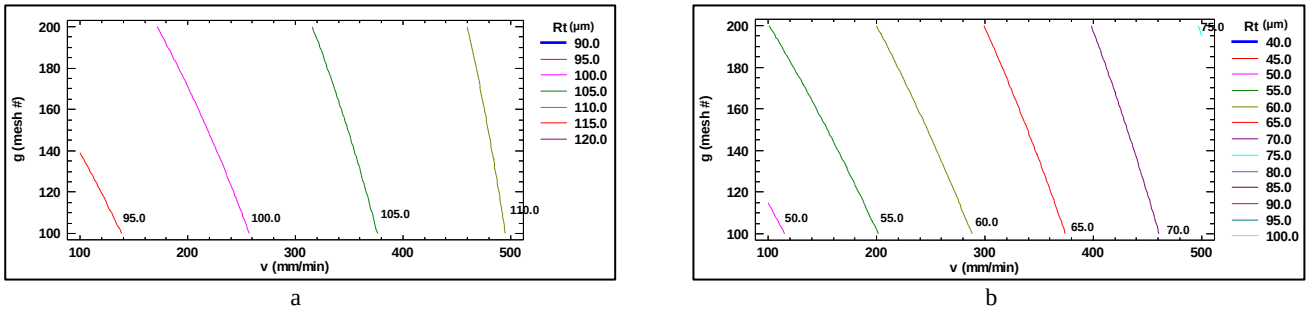

a b

Figure 12. Constant level curves *Rt* versus *v* and *g* at *D* = 0.76 mm and q_a = 180 g/min (**a.** bottom zone, **b.** top zone)

4. Conclusions

After carrying out the experimental program, the following more important conclusions can be summarized:

-there is a major difference between the values of both roughness parameters investigated for the two characteristic areas of the cut, kerf zone being the factor with the greatest influence;

-the most effective way of improving both roughness parameters is to decrease traverse speed, but this decision negatively influences AWJC efficiency [19];

-as a result, a proper choice for obtaining benefits regarding surface finish, avoiding a significant decrease of material removal rate [19], is to use a lower diameter of the focusing tube;

-empirical models were found, having *R*-Squared values greater than 90%, which enable the estimation of roughness height parameters for both kerf zones, in the selected experimentation range;

-an appropriate selection of the input parameters, in order to achieve specified values of *Rz1max* and *Rt* parameters, is facilitated by the surface plots and, especially, by the constant level curves.

Acknowledgments: The author would like to thank Duqueine Composites, Timisoara, for the support given, by providing the investigated material and facilitating AWJ cutting of the specimens.

References

1. *** Kevlar® Properties. Technical Guide, DuPont™, 2019. Available online: https://www.dupont.com/news/kevlar-properties.html (accessed on 18.06.2022)
2. *** Aramid & Kevlar Composites, DEXCRAFT, 2020. Available online: http://www.dexcraft.com/articles/aramids/aramid-kevlar-composites/ (accessed on 18.06.2022)
3. *** Volkswagen Clutch Discs - California Custom Clutch. Available online: https://californiaclutch.com/product/volkswagen-performance-kevlar-kevlar-clutch-disc-solid-hub/ (accessed on 18.06.2022)
4. *** Flexible Dupont™ Kevlar® Hull. Available online: https://www.biondoboats.com/content/patented-technology/flexibile-dupont-tm-kevlar-r-hull (accessed on 18.06.2022)
5. *** Kevlar: The Polymer That Protects. Available online: https://kevlarchemistry.neocities.org/portfolio (accessed on 18.06.2022)
6. *** Kevlar® for Aerospace. Available online: https://www.dupont.com/fabrics-fibers-and-nonwovens/kevlar-for-aerospace.html (accessed on 18.06.2022)
7. JANKOVIĆ, P., RADOVANOVIĆ, M., Correlation of cutting data by abrasive water jet, Annals of *the Oradea University, Fascicle of Management and Technological Engineering*, **VII (XVII)**, 2008, 1528-1533.
8. GUBENCU, D., Tendințe în evoluția proceselor de rectificare cu control activ (Trends in the evolution of active control rectification processes), *A X-a CITN, Tehnologii neconvenționale. Prezent şi perspective*, may 2001, Timișoara, Romania, Editura Augusta, 38-43.
9. HAN, A., GUBENCU, D., PILLON, G., A Generalized Structure Based on Systemic Principles of the Characteristic Variables of Materials Laser Processing, *Laser & Optics Technology*, **37/7**, 2005, 577-581.
10. GUBENCU, D., POP-CĂLIMANU, M., Study of the Factors Influence on the Objective Functions of Wire EDM of AA2124/SiC/25P, *22nd International Conference on Metallurgy and Materials (METAL 2013)*, Brno, Czech Republic, 15-17 may 2013, 1474-1479.
11. SIDDIQUI, T.U., SHUKLA, M., Optimisation of surface finish in abrasive water jet cutting of Kevlar composites using hybrid Taguchi and response surface method, *Int. J. Mach. Mach. Mater.*, **3**, 2008, 382-402.
12. KUMAR DAHIYA, A., KUMAR BHUYAN, B., KUMAR, S., Optimization of Process Parameters for Surface Roughness of GFRP with AWJ Machining Using Taguchi and GRA Methods, *Int. J. Mod. Manuf. Technol.*, **XIII/2**, 2021, 14-20, doi.org/10.54684/ijmmt.2021.13.2.14

13. MAYUET ARES, P.F., GIROT MATA F., BATISTA PONCE M., SALGUERO GÓMEZ J., Defect Analysis and Detection of Cutting Regions in CFRP Machining Using AWJM, *Materials*, **12**, **4055**; 2019, doi:10.3390/ma12244055.
14. AZMIR, M.A., AHSAN, A.K., RAHMAH, A., Effect of abrasive water jet machining parameters on aramid fibre reinforced plastics composite, *Int. J. Mater. Form*, **2**, 2009, 37–44.
15. JAGADEESH, B., DINESH BABU, P., NALLA MOHAMED, M., MARIMUTHU, P., Experimental investigation and optimization of abrasive water jet cutting parameters for the improvement of cut quality in carbon fiber reinforced plastic laminates, *Journal of Industrial Textiles*, **48(1)**, 2018, 178–200, DOI: 10.1177/1528083717725911.
16. MANIVANNAN, J., RAJESH, S., MAYANDI, K., RAJINI, N., AYRILMIS, N., Investigation of abrasive water jet machining parameters on turkey fibre reinforced polyester composites, *Mater. Today Proc.*, **45**, 2021, 8000–8005.
17. DHANAWADE, A., KUMAR, S., Experimental study of delamination and kerf geometry of carbon epoxy composite machined by abrasive water jet, *J. Compos. Mater.*, **51**, 2017, 3373–3390.
18. KUMAR, U.A., ALAM, S.M., LAXMINARAYANA, P., Influence of abrasive water jet cutting on glass fibre reinforced polymer (GFRP) composites, *Mater. Today Proc.*, **27**, 2020, 1651-1654, doi.org/10.1016/j.matpr.2020.03.554.
19. GUBENCU, D.V., LAZĂR, C.O., Experimental modeling of abrasive water-jet cutting processes of Kevlar fiber-reinforced polymer composites, *J. Phys.: Conf. Ser.*, 2540 012044, doi:10.1088/1742-6596/2540/1/012044.
20. *** Quick guide to surface roughness measurement, Mitutoyo, 2016. Available online: https://www.mitutoyo.com/webfoo/wp-content/uploads/1984_Surf_Roughness_PG.pdf (accessed on 18.06.2022)
21. *** Surface Roughness Chart: Understanding Surface Finish in Manufacturing, 2011. Available online: https://www.rapiddirect.com/blog/surface-roughness-chart/ (accessed on 18.06.2022)
22. OEHLERT, G. W., *A First Course in Design and Analysis of Experiments*, University of Minnesota, 2010.

Manuscript received: 06.09.2023